Hindawi
Journal of Sensors
Volume 2017, Article ID 4879528, 5 pages
https://doi.org/10.1155/2017/4879528

Research Article

Measuring the Radial Position of Defects within Optical Fibers Using Skew Rays

George Y. Chen, Dale Otten, Yvonne Qiongyue Kang, Tanya M. Monro, and David G. Lancaster

Laser Physics and Photonic Devices Laboratories, University of South Australia, Adelaide, SA 5095, Australia

Correspondence should be addressed to George Y. Chen; george.chen@unisa.edu.au

Received 14 March 2017; Accepted 12 April 2017; Published 4 June 2017

Academic Editor: Banshi D. Gupta

Defects within optical fibers can cause premature failure in fiber-based systems and must be detected early to avoid performance degradation. Addressing this need can ensure that no defective optical fibers are being used by end users and improve processes to reduce the number of defects during manufacturing. The main challenge to date has been developing a technique that can measure defects along long lengths of fiber, within opaque packaging, and with position information. We demonstrate a simple and novel technique for detecting and radially resolving microscopic defects in packaged/buried fibers using an angle-resolved interrogator that analyzes the transmission of different ray groups. We have measured the accuracy to be as low as ±2 μm, which is sufficient for most fibers that have diameters in the order of ~100 μm.

1. Introduction

The duty of the polymer coating on an optical fiber is to protect its glass cladding against nicks, shocks, and adsorption of chemicals. In the absence of coatings, even the tiniest defect in a fiber cladding typically grows under long-term strain [1]. Eventually, the fiber may break and cause a costly system failure in its application, such as fibers deployed for telecommunications that are required to last decades [2]. Some fiber lasers use cladding-pumped double-clad fibers, which requires the coating to function as a second cladding in order to guide pump light [3, 4]. In this case, the coating quality is a critical factor in terms of uniformity and optical loss. Extra care must be taken when manufacturing soft-glass fibers, such as ZBLAN and germanate fibers. These are typically manufactured using rotational casting or extrusion and thus are more prone to defects than silica fibers. Additionally, double-clad fibers may experience imperfections during rod-in-tube integration. Hence, to prevent crack propagation, scattering, and thermal effects that can damage the fiber, any defects within the fiber, coating, and layer interfaces must be detected early and removed. Knowing the radial position of the defect(s) is valuable though not currently possible, because it gives an insight into which layer hosts the defect(s). Addressing this need allows optical fiber manufacturers to obtain detailed defect information after manufacturing, after transportation, and during maintenance. As a result, they can ensure that no defective optical fibers are being used by end users and improve processes to reduce the number of defects and improve rod-in-tube integration during manufacturing. A few techniques have been proposed over the years. One known technique [5] operates by visually analyzing the diffracted light when external surface illumination is used. Since this involves a point-by-point inspection, it is impractical for long lengths of fibers. Another known technique [6] involves internally illuminating the fiber with visible light and checking for bright specks from the outside. Again, this is not viable in outdoor environments or when the fiber has an opaque jacket. The main challenge to date has been developing a technique that can measure defects along long lengths of fiber, within opaque packaging, and with position information.

Recently, we have introduced angle-resolved skew rays as a highly sensitive interrogation technique for detecting defects within fibers and coatings [7], which works even if the fibers are packaged/buried. In this work, we extend the scope

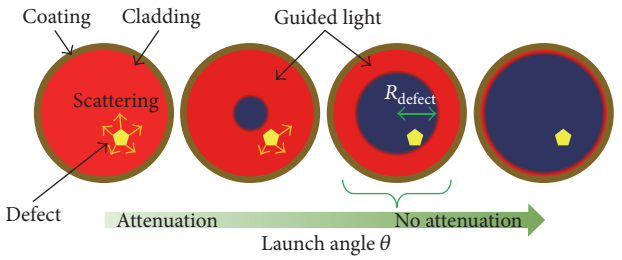

FIGURE 1: Illustration of the evolution of light content within the cross-section of an optical fiber when the launch angle of input light is varied, and the different degrees of overlap with a defect.

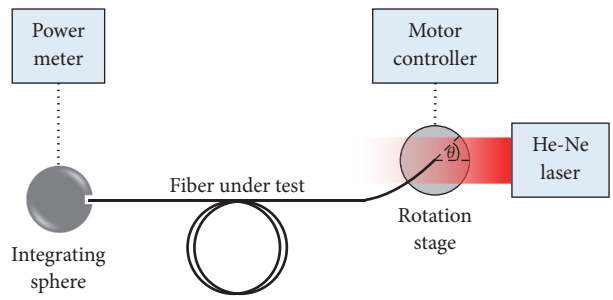

FIGURE 2: Schematic of the angle-resolved interrogation system.

of this technique by additional signal processing involving angle-dependent optical loss to measure the radial position of microscopic defects within fibers.

2. Theory

Meridional rays turn into skew rays [8] when they reflect off the curved geometry of a cylindrical multimode fiber. Skew rays propagate in a helical pattern along the fiber axis, which naturally establishes a circular coverage of possible defect-induced absorption and/or scattering. They also exhibit a larger number of reflections per unit length than meridional rays. These two factors make skew rays far more sensitive than meridional rays to defects of arbitrary size and geometry within the fiber and/or coating. Hence, for identifying coating defects, high-order skew rays are ideal. Sensing coating defects [7] and external refractive indices [9] have been recently demonstrated based on this concept. However, for identifying fiber defects, the ideal skew ray order depends on the defect position. This is because all rays interact with the outer boundary at some point, but not necessarily the entire inner space. As shown in Figure 1, increasing the launch angle (θ) of incident light converts the guided light into an ever-thinning ring beyond the acceptance angle for the fiber. In any case, the basic signs of attenuation from the angle-resolved data informs that defect(s) are present, and thus the optical fiber needs replacement. A new and effective way for determining the radial position of a defect is based on finding θ that prevents the guided rays from interacting with the defect and then deriving the corresponding radial position using ray-optics theory.

This angle-resolved interrogation technique needs to scan different θ (i.e., different ray groups) for optical loss in the measured data of the defective fiber when compared with that of the pristine fiber. To deliver the most sensitive observations that depend on the nature of the defect(s), the structure of the fiber, and the specifications of the light source, the collection of data points from different θ must be analyzed to find the corresponding θ. To distinguish defect-induced attenuation from changes in the laser source, this swept-angle approach must be used to isolate discrepancies.

The radial position of fiber defects relative to the fiber center in a cladding-oriented model is estimated by analyzing the lowest value of the range of θ that results in negligible attenuation. For simplicity, it is assumed that (a) there is no core/pedestal; (b) the core/pedestal is relatively small such that its ray contribution is negligible; and/or (c) the coating is very lossy and skew rays do not transmit through. As a result, the radial position can only be determined for the fiber, not its coating.

The outermost position of defects (R_{def}) relative to the fiber center can be derived from the doughnut ratio of the near-field profile of light [10]:

$$R_{def} = R_{clad} \sin\left[\cos^{-1}\left(\frac{n_1}{\sin\theta}\cdot\cos\left[\sin^{-1}\left(\frac{n_2}{n_1}\right)\right]\right)\right], \quad (1)$$

where R_{clad} is the radius of the cladding and n_1 and n_2 are the refractive indices (RI) of the core and cladding, respectively. To produce physically meaningful positions, the observed and input θ must be greater than or equal to the acceptance angle of the cladding-coating interface. This is always the case, because only beyond the acceptance angle would the meridional rays start leaking out of the fiber that generates a centralized blind spot to defects.

3. Setup

The interrogator is described in Figure 2. To excite the fiber under test (FUT), an unpolarized single-mode He-Ne laser source (Thorlabs HNLS008R-EC) was used with a wavelength of 632.8 nm. To provide a uniform intensity distribution, the beam excites the FUT with a spot diameter about five times larger than the cladding diameter of the FUT. The FUT was mounted on a motorized rotation stage (Thorlabs CR1/M-Z7) such that the end-face was positioned at the center of rotation. Although skew rays can also be generated from focused light from a lens, the contribution from low-order skew rays limits the sensitivity as it reduces the total number of reflections, as well as being alignment critical and geometrically unstable. The transmitted rays were collected by an integrating sphere (Thorlabs S142C) connected to a power meter (Thorlabs PM100A). The light entering the fiber between the end-face and the coating strip-edge is mostly leaky due to the refraction of light and thus the conversion into significantly higher-order rays. Hence, the length of this section is not important. To compensate for the reduced input power from the Lambertian angle effect, a division by the cosine of θ was applied that achieves a flat-top angle-resolved power profile when the FUT has low loss. No compensation was needed for the angle-dependent

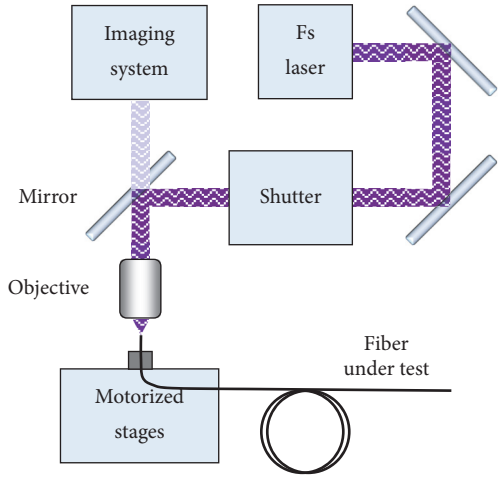

Figure 3: Schematic of the femtosecond-laser material-processing system.

reflectivity, because its contribution at $\theta < 45^\circ$ is negligible. These effects shape the profile but do not influence the attenuation caused by defects.

The FUTs were all taken from a spool of silica fiber with a core diameter of 10 μm, pedestal of 30 μm, cladding diameter of 200 μm, cladding/coating diameter of 300 μm, and a fiber length of 1 m. The RI of the cladding and coating at 633 nm wavelength is 1.457 and 1.409, respectively. Note that longer fibers can be used as long as the received power is above the noise floor of the power meter.

The optical loss associated with different launch angles or ray groups propagating along a specific optical fiber can be very different. From angle-resolved cut-back measurements, the optical loss of the propagating skew rays at $\theta = 0^\circ$ (0 NA) is 0.03 dB/m, at $\theta = 5.7^\circ$ (0.1 NA) is 0.03 dB/m, at $\theta = 11.5^\circ$ (0.2 NA) is 0.05 dB/m, at $\theta = 17.5^\circ$ (0.3 NA) is 0.1 dB/m, at $\theta = 23.6^\circ$ (0.4 NA) is 0.2 dB/m, at $\theta = 30.0^\circ$ (0.5 NA) is 0.34 dB/m, at $\theta = 36.9^\circ$ (0.6 NA) is 0.52 dB/m, and at $\theta = 44.4^\circ$ (0.7 NA) is 0.78 dB/m. With the optical power of the laser source being 0.8 mW and the detection limit of the power meter being 1 nW, the light can be attenuated by up to 59.0 dB. With the maximum attenuation divided by the maximum optical loss of 0.78 dB/m, the maximum fiber length is 75.7 m. To increase the maximum fiber length, a light source with higher optical power can be used, the collimated spot size can be reduced for higher intensity or higher coupled-power, and/or a power meter with a lower detection limit can be used.

To create fiber defects at specific locations in the FUT for validating our technique, an in-house femtosecond-laser material-processing system was used to inscribe defects resembling a microsphere with an altered RI to its surroundings. In comparison, air bubbles imparted during fiber drawing are even more visible, as higher RI contrast scatters light more strongly. The femtosecond-laser material-processing system (i.e., 1047 nm wavelength, 250 fs pulse width, 1.0 MHz repetition rate, 1.0 μJ pulse energy, 0.8 NA infinity-corrected microscope-objective lens, 50x magnification, and 1 mm working distance) is shown in Figure 3. This pulse repetition rate provides high peak-intensities, while retaining a weak thermal process in which laser-induced modifications in the fiber are spherical. The pulse energy was controlled by a variable attenuator (i.e., included in the drawn laser module) and two thin-film polarizers in series. Bursts of laser pulses were controlled by a mechanical shutter with a throughput timeframe of ~30 ms.

To adjust the position of the fiber defect relative to the microscope-objective lens, motorized 4-axis air-bearing translation stages of ~100 nm accuracy were used. To align the focal spot within the FUT and check the fabricated defect, an imaging system was mounted above the objective lens. The imaging system consists of a color CCD camera (i.e., Edmond Optics EO-5012C) fitted to a 50 mm variable focal length lens (i.e., Navitar NMV-50M1). The lens input is placed at ~250 mm from the back aperture of the objective lens. The mirror noted in Figure 3 is a dichroic mirror that reflects a narrow wavelength band around the laser wavelength and transmits the bulk of the remaining light to the imaging system. In this configuration, the imaging system in conjunction with the objective lens forms a simple microscope with the same field of view as the laser. The defect of each FUT can be located anywhere along the length of the fiber, even within the section inside the integrating sphere. This is because the integrating sphere has a blind spot aligned with the direction of backscattered light. Therefore, a large portion of the rays leaking out of the fiber due to the defect will not be collected and thus produces a detectable signal change.

4. Measurements

After the defects were inscribed into the FUTs, the radial position of the defect from the fiber center was determined with a microscope under 20x magnification. Figures 4(a) and 4(b) show one FUT with a defect written at the end-face surface (i.e., ablation due to weak thermal dissipation) at an observed outermost radial positon of $R_{\text{def,obs}} = 12 \pm 3\,\mu$m. The side-illumination demonstrates how skew rays would scatter from encountering the defect. Figures 4(c) and 4(d) show another FUT with a defect written below the end-face surface (i.e., internal microsphere of altered RI) at $R_{\text{def,obs}} = 33 \pm 3\,\mu$m. Figures 4(e) and 4(f) depict the third FUT with a defect created much deeper from the end-face surface (i.e., internal microsphere of altered RI) at $R_{\text{def,obs}} = 121 \pm 10\,\mu$m.

The system noise amplitude was measured to be 0.10 μW over a duration of 1 min being similar to the typical measurement time. This is used as the tolerance for negligible attenuation. The measured angle-resolved data for five FUTs with different defect positions were analyzed, and the corresponding data for $R_{\text{def,obs}} = 121 \pm 10\,\mu$m is shown in Figure 5. The launch angle (θ) is converted into numerical aperture (NA = $\sin\theta$) for normalization, and it provides an easier readout of the fiber NA from where the optical power sharply declines. The attenuation exceeds 0.4 dB between $\theta = 11.5^\circ$ and 17.5° (i.e., $\theta = 0.20$ rad to 0.30 rad, NA = 0.20 to 0.30), indicating that more rays interacted with the defect and/or the defect geometry scattered/absorbed more light at that condition. However, the attenuation drops beyond $\theta = 17^\circ$

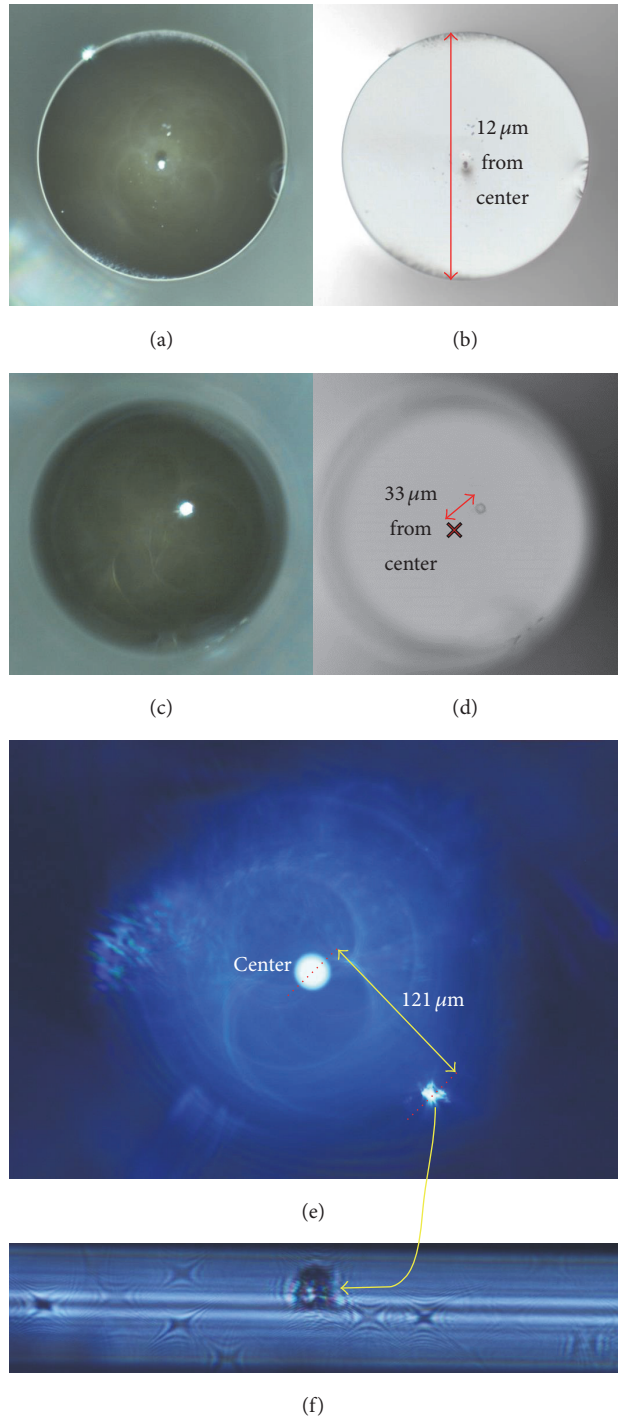

Figure 4: Microscope images showing defects within the same type of fiber at different radial and axial positions from a longitudinal perspective: (a) at 12 μm radial displacement with side-illumination, (b) at 12 μm radial displacement without side-illumination, (a) at 33 μm radial displacement with side-illumination, (b) at 3 μm radial displacement without side-illumination, (e) at 121 μm radial displacement with side-illumination, and (f) same as (e) but from a transverse perspective.

(i.e., $\theta = 0.30$ rad, NA = 0.3), reaching zero at $\theta = 27.4791^{\circ}$ (i.e., $\theta = 0.4796$ rad, NA = 0.4614), indicating that the ring of light within the fiber no longer extends far enough towards the core to interact with the defect. The data yields a measured outermost radial positon of $R_{\text{def,mea}} = 119$ μm by using (1) with $\theta = 27.4775^{\circ}$, which shows good agreement (i.e., within error bars) with $R_{\text{def,obs}} = 121 \pm 10$ μm observed by the microscope.

Figure 6 shows that the measurement of defect position is reasonably accurate considering the uncertainties, by comparing the measured ($R_{\text{def,mea}}$) and observed ($R_{\text{def,obs}}$) values

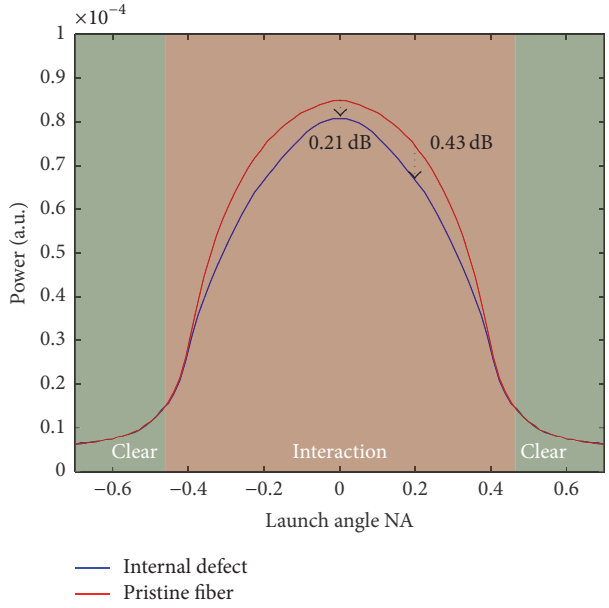

FIGURE 5: Angled-resolved data comparing a pristine FUT and one that contains an internal defect at a radial position of 121 μm.

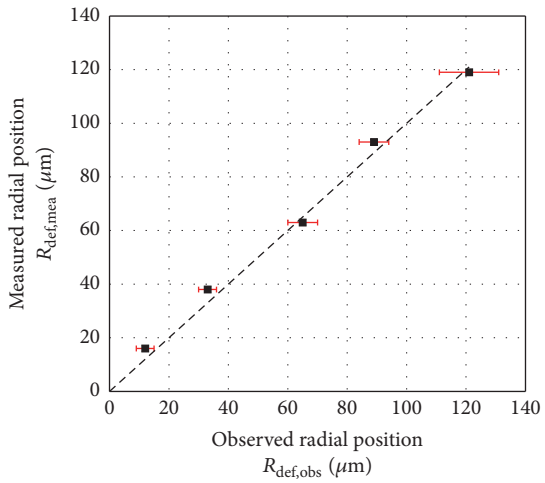

FIGURE 6: Comparison of measured and observed radial positions, with line fitting of unity gradient.

for the three cases. The minimum and maximum differences are 2 μm and 5 μm, respectively, which are mainly attributed to observation estimation.

5. Conclusions

For the first time, we can estimate the radial position of microscopic defects within packaged/buried optical fibers, by using an angle-resolved interrogation system. This is applicable to defect(s) in the core (i.e., no optical loss at medium launch angles) and the cladding (i.e., no optical loss at high launch angles), but not in the coating (i.e., nonzero optical loss, higher optical loss at higher angles). The accuracy can be as low as ±2 μm, which is sufficient for most fibers that have diameters in the order of ~100 μm. This technique would be of interest to optical fiber manufacturers who would like to check the quality of fibers and gain an insight into where and possibly how defects occur within fibers based on their radial position, in order to improve their processes.

Conflicts of Interest

The authors declare that there are no conflicts of interest regarding the publication of this paper.

Acknowledgments

Tanya M. Monro acknowledges the support of an ARC Georgina Sweet Laureate Fellowship.

References

[1] K. Watanabe and F. Ziegler, "Dynamics of advanced materials and smart structures," in *Proceedings of the IUTAM Symposium*, Springer-Science Business Media, 2002.

[2] B. Woodward and E. B. Husson, *Fiber Optics Installer and Technician Guide*, Sybex, 2005.

[3] M. N. Zervas and C. A. Codemard, "High power fiber lasers: a review," *IEEE Journal of Selected Topics in Quantum Electronics*, vol. 20, no. 5, Article ID 0904123, 2014.

[4] M.-A. Lapointe, S. Chatigny, M. Piché, M. Cain-Skaff, and J.-N. Maran, "Thermal effects in high power CW fiber lasers," in *Fiber Lasers VI: Technology, Systems, and Applications*, vol. 7195, 71951U of *Proceedings of SPIE*, Calif, USA, January 2009.

[5] S. S. Patil and A. D. Shaligram, "On-line defect detection of aluminum coating using fiber optic sensor," *Photonic Sensors*, vol. 5, no. 1, pp. 72–78, 2015.

[6] S. C. Gupta, *Textbook on Optical Fiber Communication and Its Applications*, PHI Learning Pvt., 2004.

[7] G. Y. Chen, T. M. Monro, and D. G. Lancaster, "Detection of microscopic defects in optical fiber coatings using angle-resolved skew rays," *Optics Letters*, vol. 41, no. 17, pp. 4036–4039, 2016.

[8] W. Snyder and J. D. Love, *Optical Waveguide Theory*, Chapman and Hall, 1983.

[9] G. Y. Chen, C. A. Codemard, R. J. Lewis et al., "Enhanced responsivity with skew ray excitation of reflection- and transmission-type refractometric sensors," *Optics Letters*, vol. 39, no. 13, pp. 3822–3825, 2014.

[10] G. Y. Chen, C. A. Codemard, P. M. Gorman, J. S. Chan, and M. N. Zervas, "Angle-resolved characterization and ray-optics modeling of fiber-optic sensors," *Journal of Lightwave Technology*, vol. 33, no. 24, pp. 5210–5217, 2015.